ICES Journal of Marine Science, 62: 615–628 (2005)
doi:10.1016/j.icesjms.2005.01.017

Eddy formation on the coast of North Norway – evidenced by synoptic sampling

O. P. Pedersen, M. Zhou, K. S. Tande, and A. Edvardsen

Pedersen, O. P., Zhou, M., Tande, K. S., and Edvardsen, A. 2005. Eddy formation on the coast of North Norway - evidenced by synoptic sampling. – ICES Journal of Marine Science, 62: 615–628.

In order to resolve advection, migration, and *in situ* population dynamics of zooplankton and capelin larvae in a mesoscale physical setting on the coast of North Norway, an extensive field survey was conducted. This paper reports on the physical conditions in the area and lays the basic environmental understanding for the analysis of vital rates of the biological components studied. We used a towed wing (SCANFISH) equipped with sensors and Objective Analysis for interpolation of hydrographic data into continuous fields. We show the importance of the mixing process along the coast of Norway, and identify the weakening of the signatures of Atlantic Water (AW). We also described the presence of a distinct and isolated water mass that is neither Norwegian Coastal Water (NCW) nor AW. This water mass had intermediate salinity but was significantly colder than NCW and AW. Several distinct non-linear mesoscale eddies were observed during a 12-day period. Anticyclonic eddies had lower salinity, while cyclonic eddies were relatively saline. We also observed meanders further offshore. Elongated eddies with the principle axis parallel to the shelf break developed into relatively larger isotropic eddies. The evolution of the eddy field was examined by cross-correlation between different periods of the survey. The most significant observation is the indication of eddy transport along the shelf. The translation speed was approximately 7 km day^{-1}. We propose that the observed features are formed by baroclinic instabilities of the Norwegian Coastal Current (NCC) and that they play a crucial role as transport agents for biota.

Keywords: mesoscale eddies, objective analysis, synoptic sampling.

Received 16 April 2004; accepted 18 January 2005.

O. P. Pedersen, K. S. Tande, and A. Edvardsen: Norwegian College of Fishery Science, University of Tromsø, 9037 Tromsø, Norway; M. Zhou: Department, University of Massachusetts Boston, Boston, MA 02125, USA. Correspondence to O. P. Pedersen: tel: +47 77646036; fax: +47 77646020; e-mail: olepp@nfh.uit.no.

Introduction

The multidisciplinary research programme "Capelin and herring in the Barents Sea – coexistence or exclusion" (BASECOEX) is aimed at establishing new understanding of capelin and herring interactions in the Barents Sea. We seek to investigate the apparent linkage between the species and investigate the possible predatory role of herring on capelin larvae through a coherent series of mesoscale field surveys and laboratory based experiments. Major topics to be addressed include: (i) the effect of physical forcings on the drift of capelin larvae and their overlap in distribution with that of herring, (ii) predator–prey interactions between capelin larvae and juvenile herring, and (iii) studies of potential genetic components of spawning behaviour, thermal preferences, and recruitment success of capelin. BASECOEX has undertaken field surveys to resolve the three-dimensional advection, migration, and *in situ* population dynamic rates of zooplankton and capelin larvae in a mesoscale physical setting in the core spawning area of capelin. This paper reports on the physical conditions in the area off Finmark and attempts to describe the basic environmental conditions for the analysis of vital rates of the biological components studied in spring 2001.

The spawning sites of capelin are often found on the transition between fjords and more exposed shelf bank areas. Most of the fjords in Finnmark are broad without a shallow sill. The circulation in these broad fjords is semiclosed (Svendsen, 1995). Water exchange is due to intrusion of tidal currents, wind- and density-driven

1054-3139/$30.00

currents associated with coastal up- or downwelling events. The variations in tides attributable to the phaselag of the barotropic tide between different positions along the coast, may affect the tidal signal in different ways: as a modulation of the current to a proper tidal oscillation in other places (Svendsen, 1995). Recent model simulations of capelin larvae drift patterns demonstrate a lack of correlation between observations and model predictions whereby the model could not reproduce the oceanic larval distribution (Eriksrød and Ådlandsvik, 1997). Several explanations are possible, but the important point here is the lack of detailed knowledge about the physical conditions in the main spawning areas of capelin off the coast of Finnmark, and the need for detailed three-dimensional data covering the appropriate temporal and spatial scales of mesoscale physical features.

Although most of the investigations of mesoscale features in the region have focused on the Norwegian Shelf up to 68°N (Lofoten), much can be learned from these studies. The current pattern along the banks off North Norway is often a superposition of a shelf-edge current and mesoscale eddy fields, indicating baroclinic instabilities of a barotropic nature (Orvik and Mork, 1995). Several previous oceanographic studies along the coast of Norway have detected the formation of eddies, rings, and meanders. Ljøen (1962) and Sundby (1976) reported semi-permanent eddies over Tromsøflaket, while Eide (1979) reported an anticyclonic, topographically trapped vortex over Haltenbanken on the Norwegian Shelf. Vinger *et al.* (1981) also conducted laboratory tests simulating the Norwegian Coastal Current (NCC). They showed formation of meanders along the Norwegian coast attributable to baroclinic instability, which was related to the speed of long internal waves. Mesoscale eddies related to frontal waves were shown in a study by Mork (1981). These waves were probably governed by baroclinicity and bathymetry. Focusing on the Lofoten area, McClimans and Nilsen (1991) made an experimental set-up in a laboratory. They observed how the NCC flows slowly northeast, containing an abundance of mesoscale eddies. However, they did not address causes or additional details of these features, and few data sets were available for comparison and verification of the simulations at that time. In the frontal system of the NCC south of 62°N, mesoscale meanders and eddies 40−100 km in diameter have been reported (Johannessen *et al.*, 1989). The same features are also observed to a lesser degree on the central Norwegian Shelf north of 62°N (Audunson *et al.*, 1981). Mesoscale meanders in the NCC with wavelengths of 5−100 km and northward propagation speed of 10−20 cm s^{-1} have been observed in satellite infrared images (Johannessen and Mork, 1979). Sætre (1999) reported meanders and the presence of mesoscale eddies at the shelf edge in the frontal zone north of 62°N along the shelf edge, along with numerous bank areas with Taylor columns. This is a region with strong currents, and it is likely that these eddies were transported along with the current. As demonstrated above, formation, extent, and propagation of eddies can have many explanations, spatial scales, and velocities. Our study field survey demonstrated a number of mesoscale eddies, and we attempt to resolve spatial scales, translation, velocities, and causes through a quasi-synoptic approach. This supersedes previous studies.

Eddies have been detected by the use of lagrangian drifter experiments (Poulain *et al.*, 1996), traditional CTD casts (Sundby, 1984), current meters (Eide, 1979), and satellite imagery (Bruce, 1995). In this study, we used a towed, undulating instrument platform, equipped with a wide range of sensors to reveal the dynamics of eddies on the spawning ground of capelin off Finnmark. The advantage of this platform is the possibility to perform 3-D semi-synoptic sampling of a bounded region. Integrating high-resolution sampling equipment onto a towed body allows quasi-synoptic studies over hundreds of squares of kilometres and throughout the full depth of the water column. We also extend previous studies by applying Objective Analysis in the processing of field data.

The objectives of the present paper were to study the formation, propagation, and variability of mesoscale eddies along the coast of North Norway.

Material and methods

Survey site and survey

The study was performed in the coastal area off Finnmark County, northern Norway (Figure 1A). This region is a part of the Norwegian Shelf. The continental shelf bathymetry off northern Norway is generally dominated by a number of relatively small and well-defined banks separated by troughs 300−400 m deep. The region investigated is Sværholthavet, located at the common inlet of Porsangerfjord and Laksefjord (Figure 1A). The depth varies from approximately 45 m to 350 m. The bathymetry at Sværholthavet is characterized by a relatively flat area, with a seamount in the middle of the common inlet rising to 45 m. On the seaward border of the study area, a similar seamount rises to above 250 m. Otherwise, the study area is characterized by a steep shelf break falling off to 250 m, followed by a relatively flat area in the range 250−300 m (Figure 1B).

The sampling area was chosen to serve the main objectives in BASECOEX. Two criteria were of particular importance: (i) high concentration of newly hatched capelin larvae and (ii) a reasonable vicinity to the herring aggregations in the southern Barents Sea off the coast of Finnmark County (I. Røttingen, pers. comm.). To the east of North Cape, high concentrations of capelin larvae were found during the initial stage of the field survey. It was then decided to study a region centered between North Cape and Nordkyn, covering both sheltered, coastal and Barents Sea water masses.

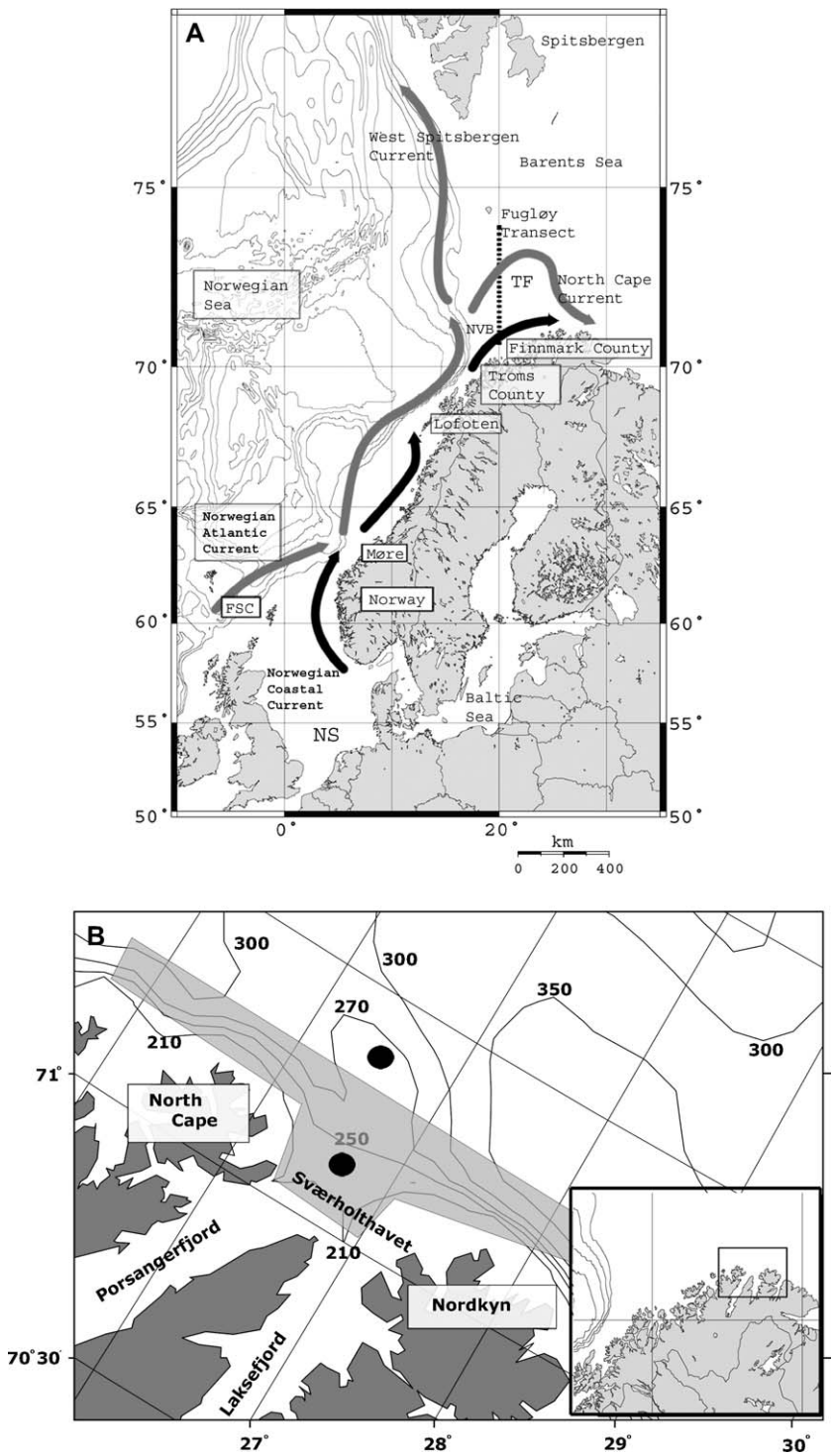

Figure 1. A) Map of the coast of Norway depicting the major current systems and geographic locations. FSC = Faroe−Shetland Channel, TF = Tromsøflaket, NVB = Nordvestbanken, NS = North Sea. The Fugløya Transect is shown by the black dotted line. B) Map of the coast of Finnmark County depicting the survey area covered (gray shaded polygon). Black circles = Seamounts. The insert is a blow-up of the coastline, and the black square in the insert shows the overall study region.

The study was conducted from 17 to 30 May 2001 in three phases (17−21 May, 21−24 May, and 25−30 May) which covered the same area (Figure 1B). Transects followed an east−west direction, with 6−11 main transects, separated by ~6.5 km and connected together at alternate ends. Owing to the shape of the survey area, transects were not of equal length and ranged from 22 to 103 km. During the first phase, only six transects were completed, because of gear malfunction.

Methods

We collected data using a towed SCANFISH (MacArtney Inc., Esbjerg, Denmark) equipped with an SBE911+ conductivity−temperature−pressure sensor (CTD; Sea-Bird Electronics Inc, Washington, USA) and a 1T Optical Plankton Counter (OPC; Focal Technologies, Dartmouth, Canada). The towed instrument platform was deployed behind the RV "Jan Mayen" (Tromsø, Norway) on a conducting tow cable and vertically undulated from 3 to 100 m. The data collected include pressure, conductivity, temperature, fluorescence concentration, and zooplankton size and counts. We also performed conventional sampling of hydrography and plankton at nine stations covering the survey area using an SBE911 conductivity−temperature−depth−fluorescence sensor (CTDF; Sea-Bird Electronics Inc, Washington, USA) and a Multiple Opening and Closing Net and Environmental Sampling System (MOCNESS; Wiebe *et al.*, 1985) with a net mesh size of 180 μm.

Data processing

To remove erroneous measurements and to smooth the physical fields, we divided the water column into 5-m bins with the first bin located between 2.5 and 7.5 m. The mean and standard deviation (s.d.) were calculated for each bin for each variable. Measurements outside 2 s.d. were discarded, and the mean recalculated. This value was used for interpolation.

For interpolation and smoothing of the measured field, Objective Analysis (OA) was applied (Gandin, 1963; Bretherton *et al.*, 1976). OA is basically a contemporary synonym for statistical estimation based on the Gauss−Markov theorem. The correlation function applied in this study is the same as in Zhou (1998). The major advantage of OA is that the method yields an estimate at every point (x, y, z, t) optimal to the least square error. Along with the interpolated field, an error field is calculated. With this method, the search radius can also be specified as an elliptic function. This is especially useful in anisotropic physical fields. In this study, a search radius of the 30 nearest data points was applied. Increasing this value further did not provide any major improvements in the interpolated fields, while smaller search radii did not produce sufficiently smooth fields. Based on the filtered and interpolated fields, we calculated the geostrophic current for the entire water column. We used 100 m as reference layer because this was our maximum sampling depth.

Results and discussion

Current systems along the Norwegian coast

Along the Norwegian coast, two major current systems dominate. These are the Norwegian Atlantic Current (NAC) and the baroclinic NCC (Sætre and Mork, 1981; Sætre *et al.*, 1988). The NAC enters the Norwegian Sea through the Faroe−Shetland Channel (FSC), containing Atlantic Water (AW). When AW enters the Norwegian Sea, the temperatures are in the range 6−9°C, and the salinity ranges between 35.1 and 35.3. Further north, in the Spitsbergen area, the temperature of the AW has fallen below 5°C, while the salinity is below 35.15 (Blindheim, 1990). The NCC consists of Norwegian Coastal Water (NCW), originating primarily from the freshwater outflow from the Baltic Sea and freshwater discharge from Norway. NCW is characterized by salinities and temperatures lower than 34.5°C and 5.5°C (Ljøen and Nakken, 1969). This water is further mixed with North Sea Water (NSW) and AW. The NCC and NAC converge in the southern part of the Norwegian Shelf, and flow northwards in parallel, the NCC inshore. Further north, outside Troms County, the NAC splits and changes name. One branch follows the shelf edge northwards, and is termed the West Spitsbergen Current. The other branch, now termed the North Cape Current, flows around the bank Tromsøflaket and continues along the Norwegian coast along with the NCC. The NCC varies seasonally in magnitude with net currents between 15 and 40 cm s^{-1} (Breen, 1990). The current directions and velocity vary with depth. Near the surface, the current is modified by winds, which are mostly from NE during summer and SW during winter (Svendsen, 1995). In our study area, these two different water masses are present and interact. In general, the AW becomes colder and fresher with increasing latitude. This is due to the mixing with NCW, which is colder and fresher, and the decrease of solar irradiance at increasing latitudes.

Hydrographic conditions in our study area

Plots of temperature vs. salinity from all points of observation are presented in Figure 2A, which gives a view of the different water masses in the area. As expected, two main water masses are observed: NCW and AW. The temperature is in the range 3.2−5.8°C, while the salinity is in the range 33.7−34.9. NCW originating from the NCC is recognized by low salinity and low temperatures (Figure 2A; left box). The warmer water has elevated salinity, and this is formerly AW, originating from the NAC (Figure 2A; right box). However, during the advection from the confluence region west of Møre, considerable mixing has occurred and the characteristic parameters of both water

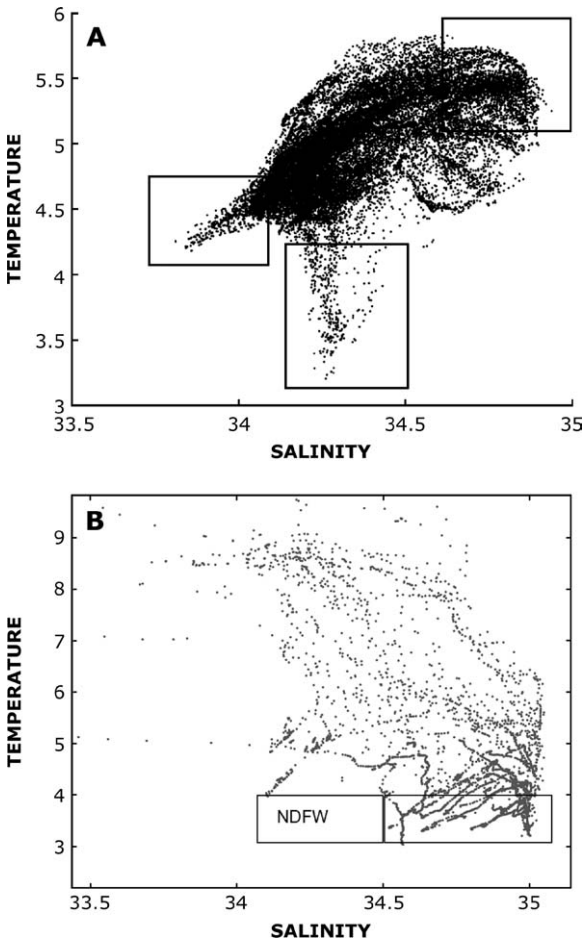

Figure 2. A) TS-diagram for all measurements collected during all phases of the cruise. The left box indicates typical coastal water masses that are fresh and cold. The right box indicates typical Atlantic water masses that are warm and saline. The middle box indicates a water mass that is cold (3.2−4 °C) and relatively saline (34−34.5). This specific water mass is defined as Norwegian Deep Fjord Water (NDFW). This water mass was restricted to a very limited area and time period. B) TS-diagram for all measurements collected by the Institute of Marine Research in Norway in 1997 covering our study area. The left rectangle delimits NDFW, while the right rectangle delimits water masses with same temperature, but higher salinity.

types have been altered. The salinity of AW has decreased to below 35.0 and a similar transition of signature has occurred with respect to temperature, recalling a temperature range of 6−9 °C in the FSC, and 5 °C further north. In between AW and NCW, there is a considerable amount of intermediate water, carrying signatures from both sources, modified by heat exchange with the air and mixing process along the coast of Norway. These results are in agreement with previous studies along the coast of Norway. The signatures of NCW were also found by Ljøen and Nakken (1969). Their observations, in the range 4.0−5.5 °C and salinities below 34.5, coincide with results from our study. The physical conditions along the Fugløya transect, which is fairly close to our study site, were investigated by Rey (1981). He found an absence of Atlantic water (>35.0) throughout the whole spring season. However, a prominent transition layer was found (salinities between 34.5 and 35), which is also consistent with results from this study (Figure 2A). This again highlights the importance of the mixing process along the coast of Norway, and the weakening of the signatures of AW.

One of the most conspicuous features observed in this field study is a water mass that is neither within the definition of NCW nor AW (Figure 2A; middle box). It is characterized by salinities between 34 and 34.5 and temperatures in the range 3.2−4 °C, which is considerably colder than NCW and AW. This water mass was found in a very confined region (Figures 3C; 4A, C; 5C). We hereby define it as Norwegian Deep Fjord Water (NDFW). Owing to the fact that salinity contributes most to the density of a water body, the signature of this water mass is vague with respect to density (Figure 4C). However, considering temperature exclusively, the signature is stronger and better defined (Figures 4A and 2A). Previous studies from the Fugløya transect show relatively cold surface waters (<4 °C) (Rey, 1981). However, these measurements were done one month prior to our field study, and the surface water is expected to be colder owing to reduced irradiance. The cold surface water from this previous study was attributed to lateral spreading of NCW. Such a lateral mechanism is known from other studies along the Norwegian Shelf (Pedersen *et al.*, 2000). The deeper regions along the Fugløya transect show no sign of NDFW (Rey, 1981). Other studies from Nordvestbanken and adjacent shelf areas also show no sign of NDFW (Nordby *et al.*, 1999). Even in March, in winter conditions with generally reduced temperatures, there were no measurements which were consistent with our observations. During 1997, the Institute of Marine Research (IMR) in Norway conducted numerous field surveys in our study area (Figure 2B). Yet, contrary to all expectations, not a single CTD-measurement found NDFW (Figure 2B; left box). In general, cold waters were more saline than NDFW (Figure 2B). The origin of IMR's CTD casts showing cold but more saline waters was dispersed throughout the entire study area (Figure 5C) thereby giving no conclusive evidence of the origin of NDFW. However, the lack of supporting evidence from other studies could be due to interannual variations of climatic conditions in this area, influencing mixing and formation of NDFW.

Circulation patterns

The cruise was divided into three consecutive phases and we have chosen to follow the same structure with regards to presentation of the results. In general, the circulation pattern shows a number of fundamental mesoscale physical

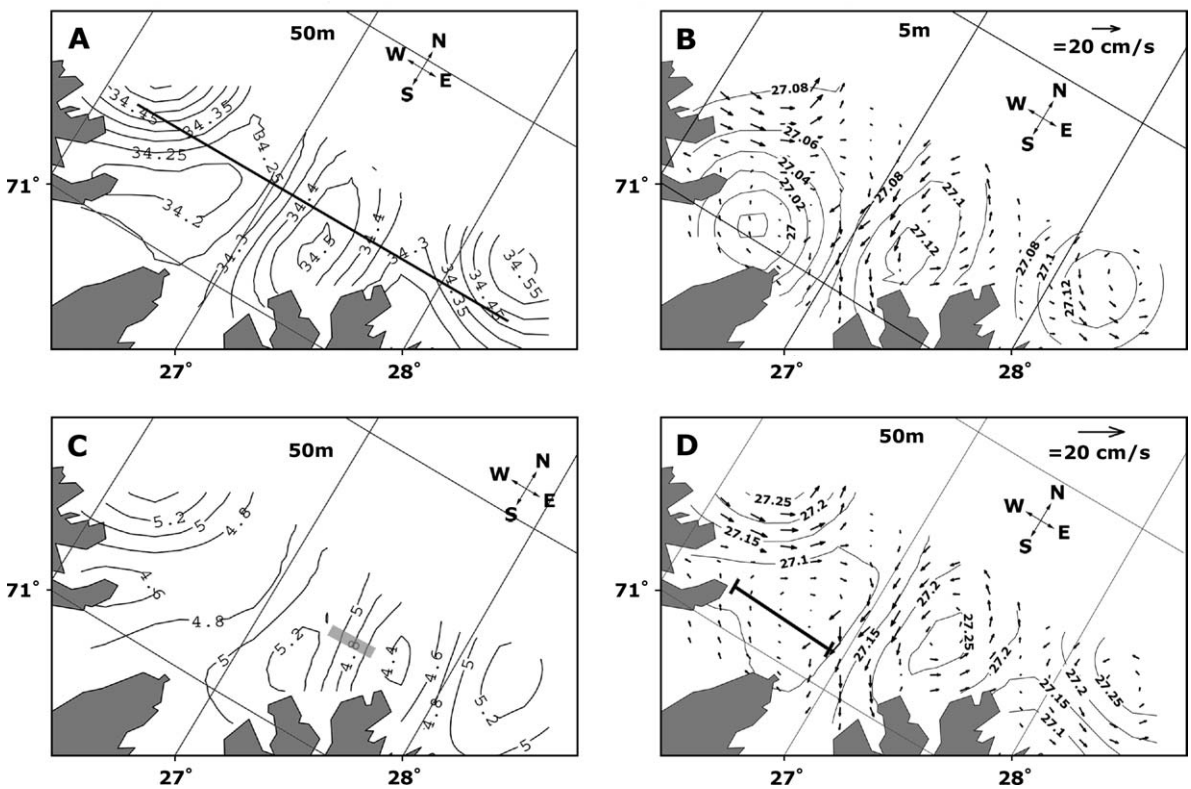

Figure 3. A) Salinity map at 50 m of the study region during phase one. Straight black line indicates transect S5. The thin solid lines indicate isolines for salinity. B) Current map at 5 m of the study region during phase one. The thin solid lines indicate isolines for σ_t. C) Temperature map at 50 m of the study region during phase one. The grey shaded area delimits a distinct water mass detected as neither NAC nor NCW. The thin solid lines indicate isolines for temperature. D) Current map at 50 m of the study region during phase one. The black segment is half-wavelength of the eddy observed. The thin solid lines indicate isolines for σ_t.

features. The current patterns during all three phases show a residual flow from west to east. However, the most distinctive mesoscale feature is the presence of strongly non-linear eddies during all three phases.

Phase one

At the mouth of the Porsangerfjord and Laksefjord, there is a distinct anticyclonic eddy (Figure 3D). This eddy is composed of water that is fresher (<34.2) than surrounding water (Figure 3A). Moreover, this obvious spatial correlation between salinity and circulation is not seen between temperature and the eddy field (Figure 3C). Mork (1981) points out that the density of coastal water is almost completely linearly related to salinity. Because we estimate the circulation pattern as a function of density, salinity and circulation will be closely related. The rotational structures observed here are well conserved throughout the water column and are seen down to 100 m, our maximum sampling depth (Figure 3D). Further east, two cyclonic eddies were observed (Figure 3B, D). Both are composed of relatively saline and warm water (>34.5, >5.2°C). In general, a significant proportion of the study area is covered with cyclonic and anticyclonic eddies. The general rule seems to be that anticyclonic bodies of water are cold and fresh, while cyclonic bodies are warm and saline.

The longitudinal transect S5, which covers in part all four rotational features seen during phase one (Figure 3A) shows strong gradients of salinity, temperature, and density (σ_t) (Figure 4). From the west, it starts in an area with high salinity and progresses eastwards through a low salinity area. This is the northern fringe of the anticyclonic eddy observed at the mouth of the two fjords, and is seen as a large body of fresher water between 26.5°E and 27°E (Figure 4B). Further east at 27.2°E to 27.5°E, the entire water column down to 100 m consists of dense and saline water. This is a strong inflow of saline water or possibly a closed mesoscale eddy located between 27°E and 27.7°E (Figure 3D). The overall picture of the area shows sharp gradients of salinity and temperature. Moreover, there is a strong signature of meandering structures, possibly several mesoscale eddies with different rotational directions and with distinct salinity signatures; either fresher or more saline waters. The magnitude of the current fields calculated for phase one is in the range 0−14 cm s^{-1} in

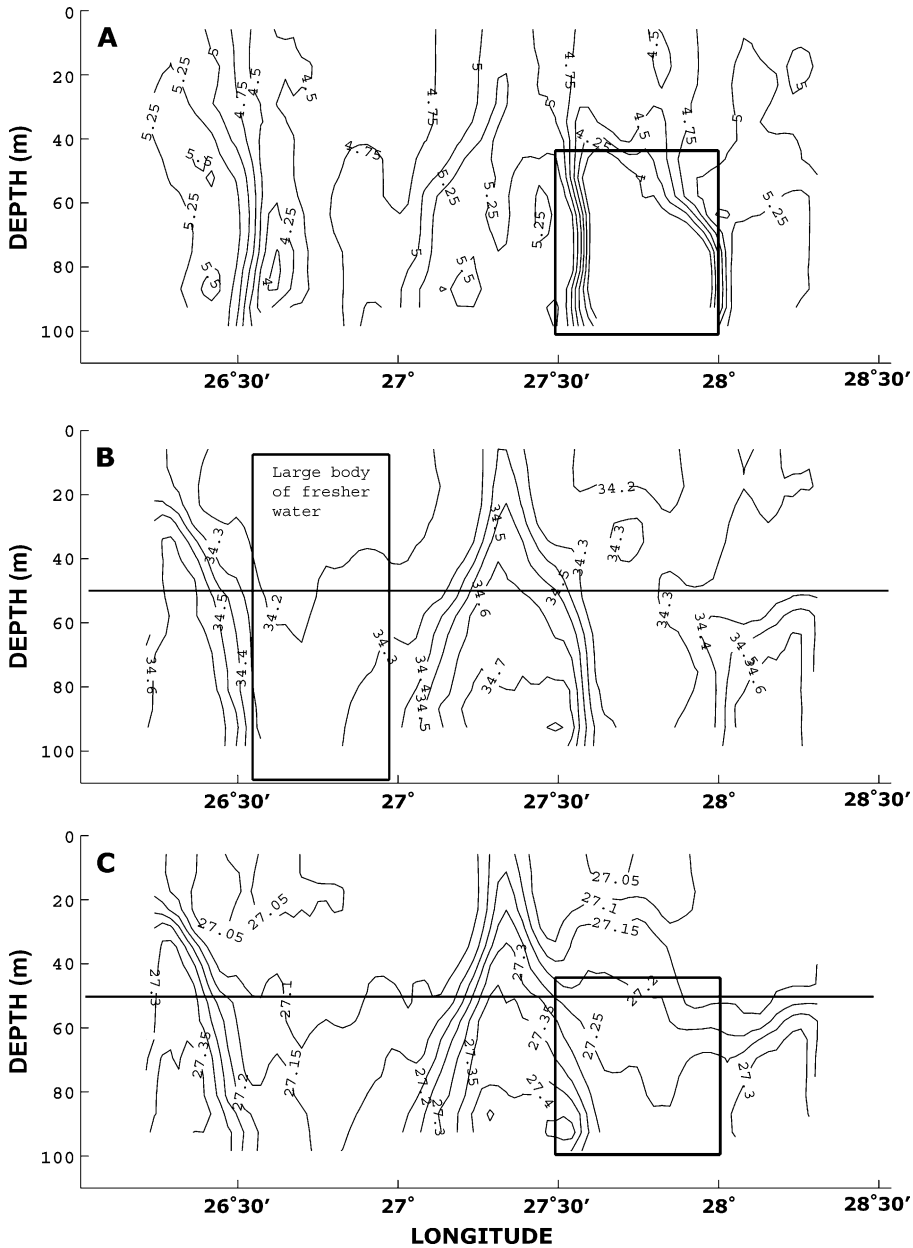

Figure 4. Temperature (A), salinity (B), and density (C) along transect S5 during phase one (S5 was the northernmost and longest transect during phase one). The black horizontal line in (B) and (C) indicates the 50 m level discussed in relation to Figure 2. The hatched rectangles in upper and lower panel indicate a distinct water mass not characterized as NAC or NCW.

the surface, while the magnitude decreases to 0−10 cm s^{-1} at 50 m. When compared with previous calculations of mean transport speed in the range 10.6−16.1 cm s^{-1} between 64°N and 68°N, the results obtained in this study have precedents in the literature (Sætre, 1999).

Phase two

Several of the mesoscale features detected during phase one were also detected in phase two. A very distinct feature observed is a cyclonic eddy at the outlet of the two fjords (Figure 5B, D). The spatial scale of this eddy is approximately the same as that found during phase one at the same location. However, the direction of rotation has reversed. The examination of the corresponding horizontal conservative properties maps shows that the eddy contains relatively saline and warm water (Figure 5A, C). The water close to the coast is in general cold and fresh, compared with the more saline, warmer water that is found further

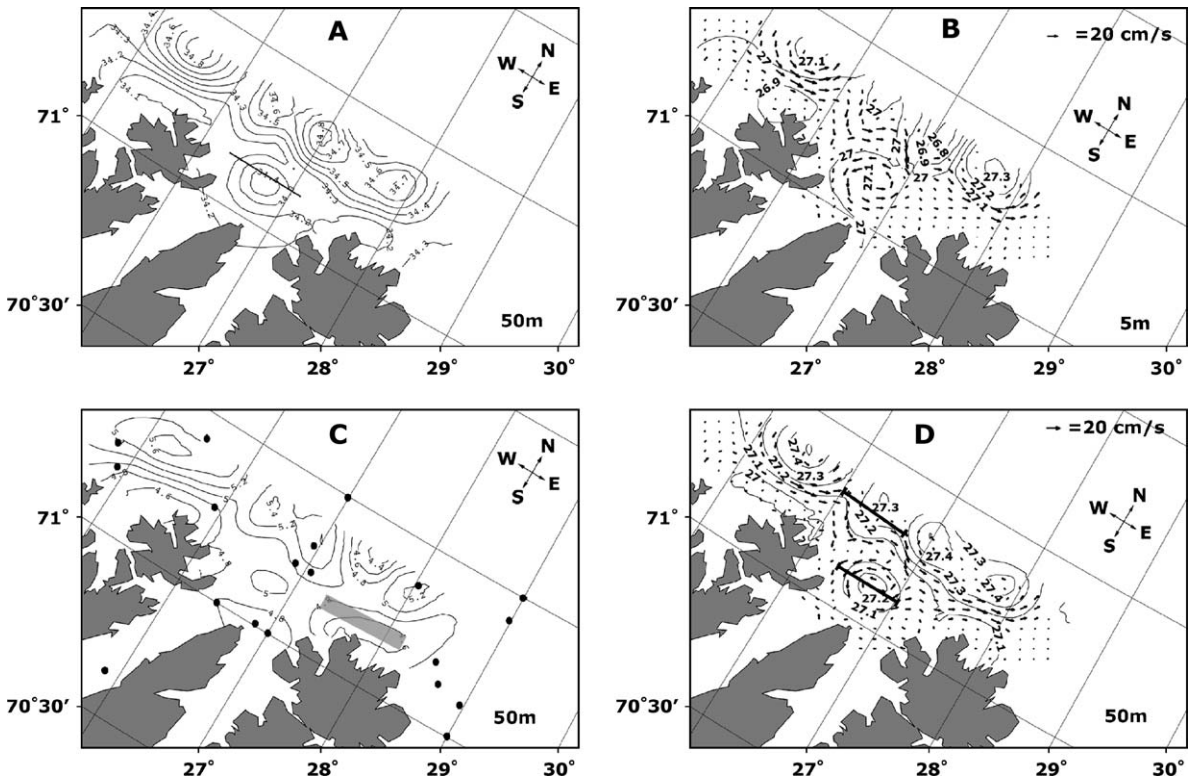

Figure 5. A) Salinity map at 50 m of the study region during phase two. Straight black line indicates transect T3. The thin solid lines indicate isolines for salinity. B) Current map at 5 m of the study region during phase two. The thin solid lines indicate isolines for σ_t. C) Temperature map at 50 m of the study region during phase two. The grey shaded area delimits a distinct water mass detected as neither NAC nor NCW. Black dots indicate positions for CTD casts taken by IMR in 1997 located in our study area. The thin solid lines indicate isolines for temperature. D) Current map at 50 m of the study region during phase two. The black segments are wavelength of observed meanders and half-wavelength of observed eddy. The thin solid lines indicate isolines for σ_t.

from the coast. However, the presence of warm and saline water in a near-coastal region shows that this is a water mass that was advected into the area between phase one and two. During phase one, there was a cyclonic rotational feature, with warm saline water, seen in the northwest region of the study area. We suggest that this mesoscale feature was advected from the west into our study region. The mapping of phase two also shows a vast number of mesoscale meandering features on the northern brink of the study area (Figure 5B, D). This is an area where the front between fresh, cold coastal waters and warm, saline Atlantic waters is found. It is possible that these structures are complete eddies, but since the features are seen on the very border of the study area, we do not have data presently to support this assumption. The northern side of the study area contains several distinct regions with saline waters (Figure 5A). These areas correlate strongly with areas containing mesoscale eddies or meanders (Figure 5B, D). These observations adhere to the general pattern of saline, warm and cyclonic eddies and cold, fresh anticyclonic eddies. The magnitude of the currents found during phase two (Figure 5B, D) range from 0 to 30 cm s^{-1} at the surface, while their magnitude decreases to 0−16 cm s^{-1} at 50 m. As was the case for phase one, the highest surface velocities are always associated with eddy structures, and they decrease with depth.

The transect T3 covers the cyclonic eddy located at the opening of the two fjords (Figure 5A). Consequently, there should be strong gradients of salinity, temperature, and density (σ_t) across the transect. The eddy signature was found between 26.5° and 27°E (Figure 6A−C). This fraction of the transect has higher salinity and warmer water, and consequently higher density. This agrees with the general notion of warm, saline and cyclonic eddies established from phase one. However, there is also a vertical gradient of the conservative properties. The salinity appears to increase with depth in this region, while the temperature has a maximum of 5.15°C at 40 m, with colder water above and below. This vertical gradient was also apparent during phase one (Figure 4B). The study area is located close to the coast, and at this time of the year, the freshwater discharge is significant due to the melting of snow. At the end of Porsangerfjord, there is a relatively big river, and we suggest that discharge from this source induces the vertical

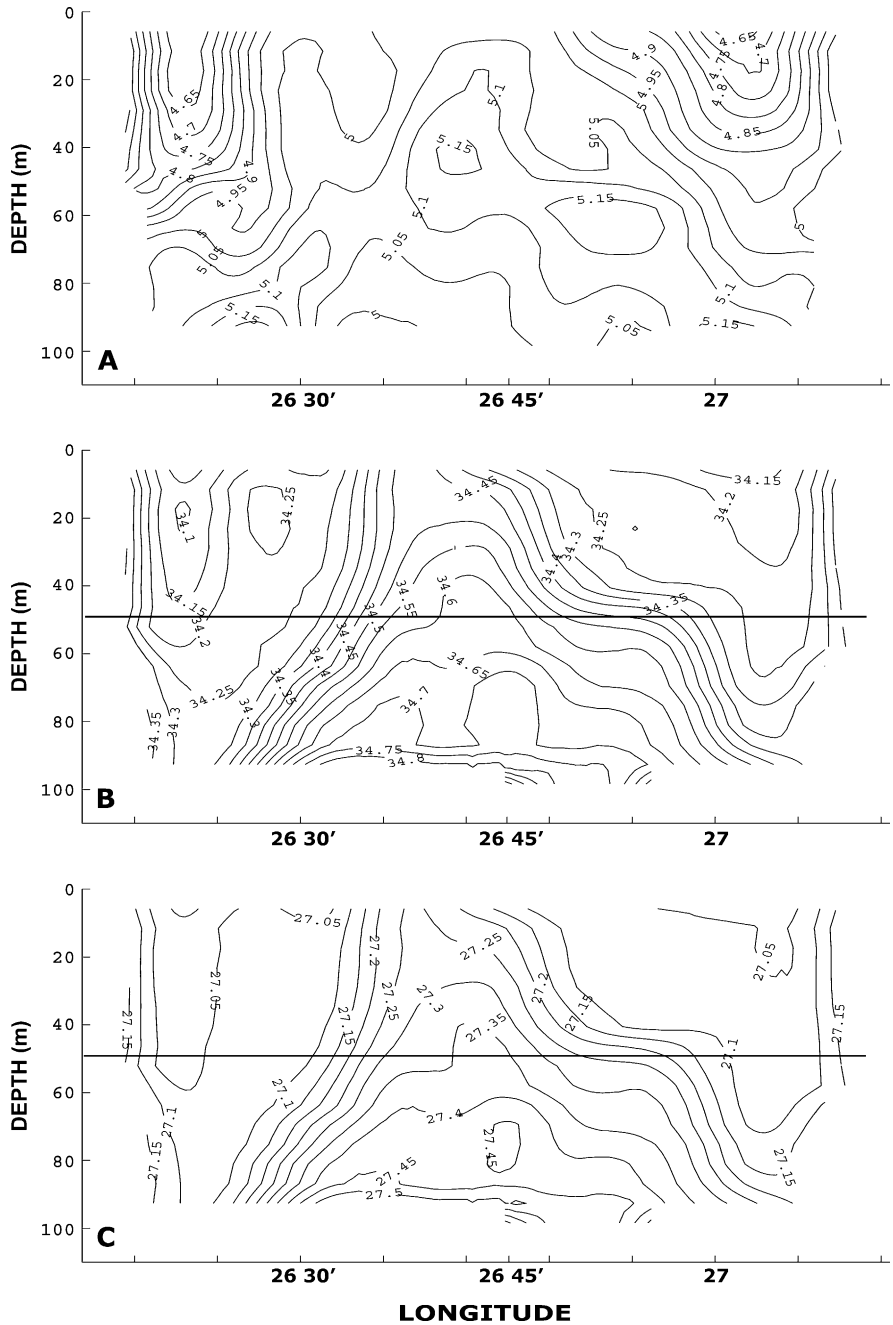

Figure 6. (A) Temperature, (B) salinity, and (C) density along transect T3 during phase two (T3 was the in the middle of the study area, and covered the outlet of the Porsangerfjord and Laksefjord).

gradients of salinity and density between 26.5° and 27°E (Figure 6B, C).

Phase three

Several of the mesoscale features previously seen were observed during the final phase of the survey (Figure 7A–D). However, relative to phase two, several significant changes had taken place. The central eddy at the opening of the two fjords had changed rotational direction to anticyclonic (Figure 7B, D). This eddy feature was produced by the cold but less saline water. The temperature of this eddy was below 4.8°C, while the salinity was below

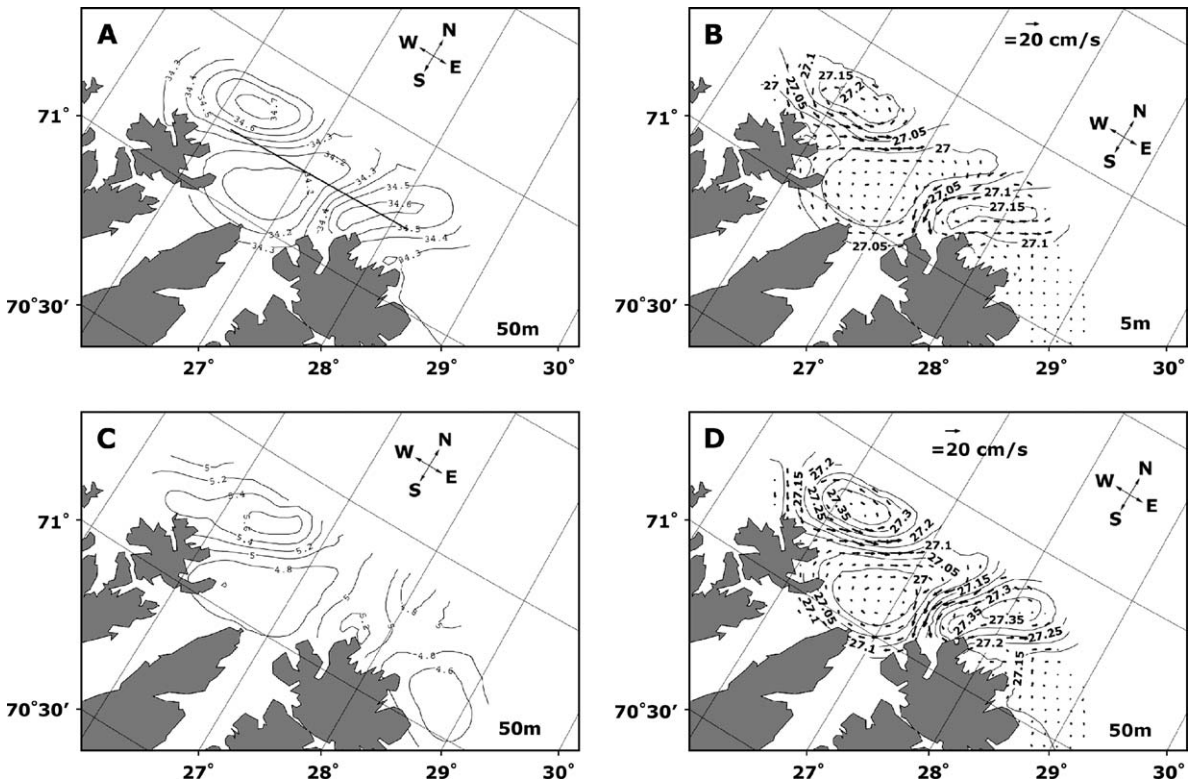

Figure 7. A) Salinity map at 50 m of the study region during phase three. Straight black line indicates transect R5. The thin solid lines indicate isolines for salinity. B) Current map at 5 m of the study region during phase three. The thin solid lines indicate isolines for σ_t. C) Temperature map at 50 m of the study region during phase three. The thin solid lines indicate isolines for temperature. D) Current map at 50 m of the study region during phase three. The thin solid lines indicate isolines for σ_t.

34.1 (Figure 7A, C). This adheres to the preceding observations of anticyclonic, fresh and cold eddies in this area. Compared with phase two, the meanders on the northern side of the study area are replaced by two larger, complete cyclonic eddies at eastern and western extremes of the study area. These eddies were saline and warm (Figure 7A, C). The magnitude of the current fields calculated for phase three ranges from 0 to 25 cm s^{-1} at the surface, and from 0 to 14 cm s^{-1} at 50 m. The highest velocities were found in two current branches; one in the western part directed away from the coast, and one in the middle of the study area, directed towards the coast (Figure 7B, D).

Spatial statistics of eddies

Spatial and temporal features of mesoscale eddies can be studied by Eulerian spatial covariances, R_S, defined as

$$R_S(x,t,r,\tau) = \langle S(x,t)S(x,t,r,\tau)\rangle, \quad (1)$$

where S represents the salinity measurements corresponding to a position x and the spatial lag r between two locations, t is the time, and τ is the time-lag between two measurements. In Equation (1), the angle brackets are the ensemble average. We make the assumption that the mesoscale variability field is homogeneous and stationary, so that the ensemble average can be substituted by the spatial average, and we have

$$R_S(x,t,r,\tau) = R_S(r,\tau) \quad (2)$$

The large scale trends in the data sets should be removed before computing the correlation functions for mesoscale features. Figures 5 and 7 show that there is no trend along the shelf break, and the salinity gradient across the shelf break direction is part of the mesoscale eddy feature. Thus, we simply removed the means of the salinity fields, and then calculated and normalized Eulerian correlation functions based on Equation (2). We chose the salinity fields at 50 m because the density fields are primarily determined by the salinity fields in our survey results (Figures 4 and 6), and the salinity field at 50 m has relatively negligible effects from surface processes and has the most distinctive mesoscale features. Because the survey during phase one covered a limited portion of the study area, we computed the auto-correlation and cross-correlation functions using only phases two and three data sets.

The change in the correlation functions shows the evolution of mesoscale features: elongated eddies with

the principle axis parallel to the shelf break during phase two developed into relatively larger and isotropic eddies in phase three (Figure 8A, B). The development of these eddies cannot be interpreted simply by the linear internal wave theories because the isohalines are nearly vertical and intercept both the surface and bottom (Pedlosky, 1998). These eddies have the solitary wave features and are strongly non-linear. Each eddy contains its water and spins while it translates along or cross the shelf break. From the potential vorticity conservation argument that water mass

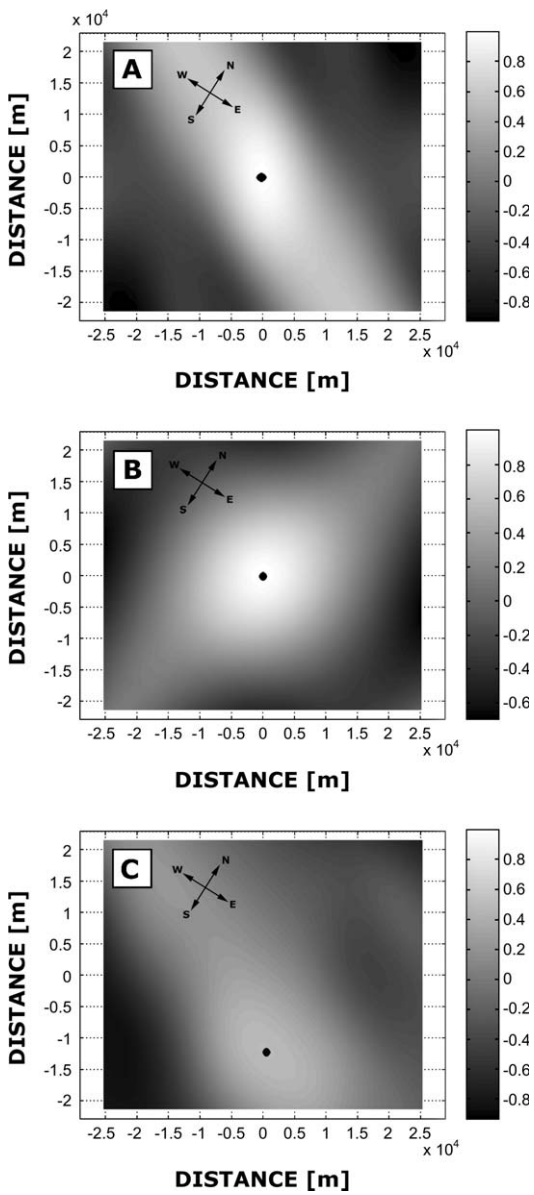

Figure 8. A) Spatial auto-correlation scales for phase two. B) Spatial auto-correlation scales for phase three. C) Spatial cross-correlation between phases two and three.

can freely translate along the isobaths, and that the slope of the bottom topography plays a role of the restoring force, mesoscale eddies can be freely stretched along the shelf break, and are relatively confined by the slope in the cross-shelf direction. In phase two of the survey, the eddy features are found along the shelf-break regions, though there is a small eddy found in Sværholthavet (Figure 5). The scales indicated by the zero-crossing in the auto-correlation function represent the effect of the shelf break. Scales in the crossing and alongshelf-break direction are approximately 15 and 40 km, respectively.

The phase three survey shows that the eddies observed on the shelf break and in Sværholthavet during the phase two survey were enlarged and translated crossing the shelf break and Sværholthavet (Figure 7). Comparing Figures 5 and 7 against the topography (Figure 1), those elongated eddies observed in phase two (Figure 5) show the effect of the shelf break, while the eddies in phase three (Figure 7) show the confinement of eddies over the local topographic features, such as the deep basin off North Cape, the shallow flat in Sværholthavet and the deep basin off Nordkyn. The eddies in phase three are nearly isotropic, with zero-crossings of 20 and 15 km in the across and alongshelf directions, respectively. The elongation of eddies in the cross-shelf direction may imply the topographic steering effect of the shallow flat in Sværholthavet.

The evolution of the eddy field can be examined by the cross-correlation function between phases two and three (Figure 8C). Because the scales of the eddy fields in phase two are smaller than those of phase three, the elongation of the cross-correlation along the shelf break direction is determined by the anisotropic feature in the auto-correlation of phase two. The most significant result in the cross-correlation function is that the maximum correlation is shifted 14 km southwards, or 10 km in both the alongshelf break southeast direction and onshore southwest direction. That is the mesoscale eddies are translating southeastwards and onto the shelf. Taking the averaged time interval of approximately 4 days between two surveys, the translation speed of these mesoscale eddies is approximately 7 km day^{-1} or 8 cm s^{-1}.

Dynamics

In this study we have established the presence of non-linear mesoscale eddies. We have also seen a high variability in position and rotational direction. This variability has also been well been documented in relation to meanders further south over the Norwegian Trench (Ikeda *et al.*, 1989). A major question is the origin of these eddies. We propose that the eddies observed in this study were advected in the NCC as isolated water masses originating further south along the coast of Norway. It is also possible that they have a significant barotropic component. Further north and east, in the central Barents Sea, their energy will eventually dissipate. However, owing to the limited coverage of our

field survey, we have no data at present to explicitly identify the area of origin. The identification of the origin would also provide a more thorough understanding of the formation of the observed eddies. In general, high energy currents like the NCC give rise to mesoscale meanders from which mesoscale eddies separate. One of the important mechanisms to generate mesoscale eddies is the baroclinic instability associated with the NCC. Mysak and Schott (1977) found evidence of baroclinic instabilities in the NCC. They investigated the NCC with the aid of a baroclinic model (Smith, 1976). Instabilities in this model had a wavelength ranging from 39 to 83 km, which agreed with observations from moorings of instabilities with horizontal length scales in the range 30–60 km. It was also shown that the fluctuations observed were in phase vertically. The vertical phase-consistency is coherent with observations of meanders and eddies from our study. During phase one in our study, a distinct anticyclonic eddy was observed in the middle of our study area. The wavelength of this eddy is approximately 40 km (Figure 3B), close to previous observations (Mysak and Schott, 1977). Further, the wavelengths of the meandering structures and eddies seen during phase two are approximately 40 and 70 km (Figure 5D), which were also seen as unstable waves in the baroclinic model.

One of the distinct feature in Figures 4 and 6 is the scales of fronts which vary from 4 to 10 km in thickness, from 4 to 15 km in the horizontal, and from 50 to >100 m in the vertical (the SCANFISH went down only to 100 m). Resolving these scales along the ship's track is the strength of the tow SCANFISH package, though these scales were not resolved in the across-shelf direction. At the latitude of our study area, taking the density difference between the cold fresh and warm saline waters approximately equal to 0.3 kg m^{-3}, and the vertical scale of a front varying from 50 to 300 m (water depth), the internal Rossby Deformation Radius (R_i) varies from 3 to 7 km, which determines the horizontal scales of fronts around the observed mesoscale eddies (Pedlosky, 1998).

Impact on biological processes

The presence of circular water movements can to a large extent perturb distribution and vital rates of zooplankton. Hernández-León *et al.* (2001) found a dramatic decrease of zooplankton biomass in the core of cyclonic eddies and higher zooplankton biomass associated with anticyclonic eddies in areas off Gran Canaria. Increased primary production caused by upwelling of nutrient-rich water has been shown in cyclonic eddies (Vaillancourt *et al.*, 2003), which in turn can raise the growth rate of the ambient zooplankton. Sánchez-Velasco and Shirasago (1999) found high concentrations of copepod nauplii and copepodites in association with mesoscale processes in the Mediterranean Sea. They proposed that this would affect the distribution of predators such as fish larvae. In a study from the Kuroshio front (Kasai *et al.*, 2002), entrainment of coastal water into a frontal eddy led to an increase in primary production. The authors concluded that this mechanism is vital for the recruitment of fish larvae in the Kuroshio system, which is supported by other investigations on production of copepods and anchovy larvae along the Kuroshio front (Nakata *et al.*, 2000; Okazaki *et al.*, 2003).

Recent studies by the first two authors (pers. comm.) support a relationship between both the composition and distribution of zooplankton and the physical properties of a region in Lake Superior. Margins of mesoscale eddy features were shown to have the highest abundance of zooplankton. Transport and survival of the pelagic stages of demersal fish and shellfish from the spawning areas to settling areas and the suitability of settling environment have generally been identified as the most crucial factors for recruitment success. From previous studies, it is known that the NCC in this area is an important carrier of pelagic eggs and larvae (Sundby, 1984). The Arcto-Norwegian cod spawns during March and April at certain locations near the coast of North Norway, with emphasis on Lofoten. The eggs are confined to the upper 50 m, depending on the conditions of the vertical mixing. Capelin also spawn nearshore along the coast of North Norway, ranging from Lofoten to East Finnmark, while haddock spawn at the shelf edge off North Norway. Capelin larvae also reside in the upper 50 m. Sætre (1999) also showed that herring on the Norwegian Shelf spawned in bank areas with quasi-stationary eddies. With the presence of mesoscale eddies in this area, and the abundance of eggs and larvae, we suggest that they act as entrainment and transport agents.

Future work

This study has shown a large number of mesoscale eddies propagating along the coast of northern Norway. The biological importance of eddies as transport agents and modulators of biological communities has been shown in several previous studies, although information from our region is sparse. The important question is whether eddies play a significant role in the transport of eggs and larvae into the nursery areas in the Barents Sea. The Barents Sea is one of the most important nursery zones for commercially important fish stocks in the world, and several of these stocks spawn in close coastal areas. Our data show that eddies have spatial scales of 15–40-km radius. However, the crucial point here is to detect explicitly the appearance of an eddy translating along the coast. Realizing that non-stationary eddies are by nature stochastic phenomena, hydrodynamical models may not be able to predict with required accuracy their position and translating velocity, which gives us a daunting task in survey planning. The operational approach would be to identify and track the eddies with the aid of satellite imagery on a continuous basis, ensuring the localization of the survey vessel within the eddy. The translating speed is approximately 7 km

a day, which enables a survey vessel to maintain its position with the eddy. However, in order to investigate discrepancies in the biological community, sufficient sampling must also take place outside the feature, but realizing the relatively low translating speed, this would enable us to sample in adjacent areas. Assuming a worst case scenario with an eddy diameter of 40 km, a realistic space scale for transects would be 80-km transect length, covering the core and surrounding areas on an outward radial track. With respect to time, sampling is mainly limited by ship availablity. However, eddies are dissipative phenomena, with a limited duration; 1–2 weeks in our region (D. Slagstad, pers. comm.). This limited time span enables us to follow at least the lifespan of one eddy, possibly several through a traditional survey. The crucial point is to track the feature through satellite imagery.

Acknowledgements

This work is a contribution to the Capelin and Herring in the Barents Sea Coexistence or Exclusion (BASECOEX) programme supported by the Research Council of Norway, contract no. 140290/140. Special thanks to Ryan D. Dorland and Y. Zhu for assistance with Objective Analysis and the crew of RV "Jan Mayen" for support on the cruise. Thanks are also due to the Norwegian Oceanographic Data Centre at IMR for providing CTD data.

References

Audunson, T., Dalen, V., Krogstad, H., Lie, H. N., and Steinbakke, P. 1981. Some observations of ocean fronts, waves and currents in the surface along the Norwegian coast from satellite images and drifting buoys. *In* The Norwegian Coastal Current. Proceedings from the Norwegian Coastal Current Symposium, Geilo, 9–12 September 1980, pp. 20–56. Ed. by R. Sætre, and M. Mork. University of Bergen.

Blindheim, J. 1990. Arctic intermediate water in the Norwegian Sea. Deep-Sea Research, 37: 1475–1489.

Breen, O. 1990. Oseanografi. Gyldendal norsk forlag, Oslo. 179 pp.

Bretherton, F. P., Davis, R. E., and Fandry, C. B. 1976. A technique for objective analysis and design of oceanographic experiments applied to MODE-73. Deep-Sea Research, 23: 559–582.

Bruce, J. G. 1995. Eddies southwest of the Denmark Strait. Deep-Sea Research, 42: 13–29.

Eide, L. I. 1979. Evidence of a topographically trapped vortex on the Norwegian continental shelf. Deep-Sea Research, 26: 601–621.

Eriksrød, G., and Ådlandsvik, B. 1997. Simulation of drift of capelin larvae in the Barents Sea. Fisken og Havet, 9. 31 pp.

Gandin, L. 1963. Objective Analysis for Meteorological Fields. Leningrad:Gridromet, English translation 1965. Israel Program for Scientific Translation, Jerusalem. 242 pp.

Hernández-León, S., Almeida, C., Gómez, M., Torres, S., Montero, I., and Portillo-Hahnefeld, A. 2001. Zooplankton biomass and indices of feeding and metabolism in island-generated eddies around Gran Canaria. Journal of Marine Systems, 30: 51–66.

Ikeda, M., Johannessen, J. A., Lygre, K., and Sandven, S. 1989. A process study of mesoscale meanders and eddies in the Norwegian Coastal Current. Journal of Physical Oceanography, 19: 20–35.

Johannessen, J. A., Svendsen, E., Sandven, S., Johannesen, O. M., and Lygre, K. 1989. Three-dimensional structure of mesoscale eddies in the Norwegian Coastal Current. Journal of Physical Oceanography, 19: 3–19.

Johannessen, O. M., and Mork, M. 1979. Remote sensing experiments in the Norwegian coastal waters. Rep. 3/79, Geophysical Institute, University of Bergen, Norway. 59 pp.

Kasai, A., Kimura, S., Nakata, H., and Okazaki, Y. 2002. Entrainment of coastal water into a frontal eddy of the Kuroshio and its biological significance. Journal of Marine Systems, 37: 185–198.

Ljøen, R. 1962. The waters of the western and northern coast of Norway in July–August 1957. Fiskeridirektoratets Skrifter Serie Havundersøkelser, 13: 1–39.

Ljøen, R., and Nakken, O. 1969. On the hydrography of the shelf waters of Møre and Helgeland. Fiskeridirektoratets Skrifter Serie Havundersøkelser, 15: 285–294.

McClimans, T. A., and Nilsen, J. H. 1991. Laboratory simulation of the ocean circulation around Lofoten from October 1982 to June 1984. SINTEF NHL report; STF60 A91027. Trondheim, Norwegian Hydrotechnical Laboratory. 28 pp.

Mork, M. 1981. Circulation phenomena and frontal dynamics of the Norwegian Coastal Current. Philosophical Transactions of the Royal Society of London A, 302: 635–647.

Mysak, L. A., and Schott, F. 1977. Evidence for baroclinic instability of the Norwegian Current. Journal of Geophysical Research, 82: 2087–2095.

Nakata, H., Kimura, S., Okazaki, Y., and Kasai, A. 2000. Implications of meso-scale eddies caused by frontal disturbances of the Kuroshio Current for anchovy recruitment. ICES Journal of Marine Science, 57: 143–152.

Nordby, E., Tande, K. S., Svendsen, H., and Slagstad, D. 1999. Oceanography and fluorescence at the shelf break off the north Norwegian coast (69°20′N–70°30′N) during the main productive period in 1994. Sarsia, 84: 175–189.

Okazaki, Y., Nakata, H., Kimura, S., and Kasai, A. 2003. Offshore entrainment of anchovy larvae and its implication for their survival in a frontal region of the Kuroshio. Marine Ecological Progress Series, 248: 237–244.

Orvik, K. A., and Mork, M. 1995. A case study of Doppler-shifted inertial oscillations in the Norwegian Coastal Current. Continental Shelf Research, 15: 1369–1379.

Pedersen, O. P., Tande, K. S., Timonin, A., and Semenova, T. 2000. A possible connection between hydrography and the distribution of *Calanus finmarchicus* on the Norwegian mid-shelf in 1997. ICES Journal of Marine Science, 57: 1645–1655.

Pedlosky, J. 1998. Ocean Circulation Theory. Springer-Verlag, Berlin. 453 pp.

Poulain, P. M., Warn-Varnas, A., and Niiler, P. P. 1996. Near-surface circulation of the Nordic seas measured by Lagrangian drifters. Journal of Geophysical Research C, 110: 18237–18258.

Rey, F. 1981. The development of the spring phytoplankton outburst at selected sites off the Norwegian coast. *In* The Norwegian Coastal Current. Proceedings from the Norwegian Coastal Current Symposium, Geilo, 9–12 September 1980, pp. 649–680. Ed. by R. Sætre, and M. Mork. University of Bergen.

Sánchez-Velasco, L., and Shirasago, B. 1999. Spatial distribution of some groups of microzooplankton in relation to oceanographic processes in the vicinity of a submarine canyon in the north-western Mediterranean Sea. ICES Journal of Marine Science, 56: 1–14.

Smith, P. C. 1976. Baroclinic instability in the Denmark Strait overflow. Journal of Physical Oceanography, 6: 355–371.

Sundby, S. 1976. Oceanographic conditions in Malangen–Fugløybanken–Tromsøflaket. An overview. Fisken og Havet, B1: 1–53.

Sundby, S. 1984. Influence of bottom topography on the circulation at the continental shelf of northern Norway. Fiskeridirektoratets Skrifter Serier Havundersøkelser, 17: 501–519.

Svendsen, H. 1995. Physical oceanography of coupled fjord-coast systems in northern Norway with special focus on frontal dynamics and tides. *In* Ecology of Fjords and Coastal Waters. Proceedings of the Mare Nor Symposium on the Ecology of Fjords and Coastal Waters, Tromsø, Norway, 5–9 December 1994, pp. 149–164. Ed. by H. R. Skjoldal, C. Hopkins, K. E. Erikstad, and H. P. Leinaas.

Sætre, R. 1999. Features of the central Norwegian Shelf circulation. Continental Shelf Research, 19: 1809–1831.

Sætre, R., Aure, J., and Ljøen, R. 1988. Wind effects on the lateral extension of the Norwegian coastal water. Continental Shelf Research, 8: 239–253.

Sætre, R., and Mork, M. 1981. The Norwegian Coastal Current, Vol. I and II. Proceedings from the Norwegian Coastal Current Symposium, Geilo, 9-12 September 1980. University of Bergen.

Vaillancourt, R. D., Marra, J., Seki, M. P., Parsons, M. L., and Bidigare, R. R. 2003. Impact of a cyclonic eddy on phytoplankton community structure and photosynthetic competency in the subtropical North Pacific Ocean. Deep-Sea Research I, 50: 829–847.

Vinger, A., McClimmans, T. A., and Tryggestad, S. 1981. Laboratory observations of instabilities in a straight coastal current. *In* The Norwegian Coastal Current. Proceedings from the Norwegian Coastal Current Symposium, Geilo, 9–12 September 1980, pp. 553–582. Ed. by R. Sætre, and M. Mork. University of Bergen.

Wiebe, P. H., Morton, A. W., Bradley, A. M., Backus, R. H., Craddock, J. E., Barber, V., Cowles, T. J., and Flierl, G. R. 1985. New developments in MOCNESS, an apparatus for sampling zooplankton and micronecton. Marine Biology, 60: 23–44.

Zhou, M. 1998. An objective interpolation method for zooplankton spatiotemporal distribution. Marine Ecology Progress Series, 174: 197–206.